PHOTOMASK

BACUS—The international technical group of SPIE dedicated to the advancement of photomask technology.

1st Place Best Poster Award - PM12

Effect of radiation exposure on the surface adhesion of Ru-capped MoSi multilayer blanks

Göksel Durkaya, Abbas Rastegar, and Hüseyin Kurtuldu, SEMATECH, 257 Fuller Road, Suite 2200, Albany, NY 12203

ABSTRACT

Better understanding of the effect of radiation on defectivity is essential to improve the stability of Ru-capped MoSi multilayer blanks. In this work, the effect of radiation exposure on the surface adhesion properties of Ru-capped MoSi multilayers was studied using optical radiation (172 nm, 532 nm, and 1064 nm). Regardless of wavelength, the surface adhesion of defects increases when exposed to radiation and scales with laser power. Changes in adhesion are compared to surface roughness. For different wavelengths, chemical modification of the surface and optical absorption of defects exhibit different contributions.

1. Introduction

In extreme ultraviolet (EUV) lithography, masks are made of EUV-absorbent patterns built on a multilayer Bragg mirror composed of 40 to 50 molybdenum-silicon (MoSi) bilayers deposited on a low thermal expansion material (LTEM) glass substrate. These masks can reflect 64% to 70% of light in the EUV region. The MoSi bilayers, or multilayers (MLs), are capped with a protective layer. Ruthenium is the material of choice for

Continues on page 3.

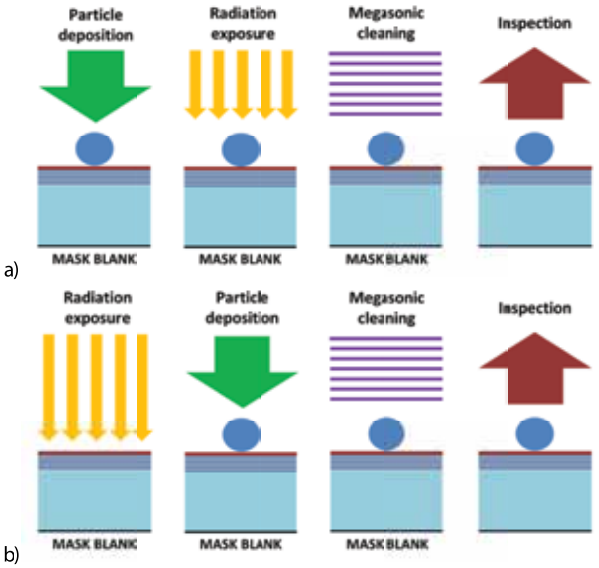

Figure 1. Experiment configurations: a) Co-exposed (Surface+particle) and b) pre-exposed (only surface) exposure experiments.

BACUS NEWS

DECEMBER 2012
VOLUME 28, ISSUE 12

TAKE A LOOK INSIDE:

SPIE

8522-39

EDITORIAL

The "Big Plates"

Oliver Kienzle, Managing Director, Carl Zeiss SMS GmbH

Although this is for sure a big impact topic, I decided to keep this editorial brief to leave even more time for thinking.

It is anticipated by many device manufacturers including logic, foundry and DRAM makers, that making EUV happen is crucial for following Moore's Law towards better performing devices at lower manufacturing costs. Although the entry point of EUV for high-volume production is delayed by the still insufficient power of the EUV source, big steps have been done towards taking full advantage of EUV:

- The EUV scanner demonstrates superior resolution figures enabling the imaging of complicated contact layer patterns.
- EUV can reduce the risk of yield issues that are expected to grow with the increasing numbers of process steps in the 193 nm multi-patterning.

Several activities are started to provide the necessary infrastructure for EUV masks including the EMI consortium funding the development of AIMS™-EUV and actinic blank inspection systems. It was shown in a wafer print study with IMEC that—within a certain size range—phase defects caused by EUV blanks can be repaired using state of the art electron beam based mask repair tools. Sematech has shown a significant reduction of blank defects as the outcome of a long term project with blank manufacturers. ASML has announced a Co-Investment Program: three chip manufacturers agreed to invest in ASML's research and development of next-generation lithography technologies over five years, specifically aimed at accelerating EUV lithography and 450 nm lithography development. Last but not least, ASML has announced to acquire Cymer. Many of us believe this is the right step to solve the source power issue in the fastest way.

With EUV projected to enter mass production for the 16 nm node in the middle of this decade, it is valid to think about the extension of EUV towards smaller nodes. Extensions of EUV are currently thought into two directions:

i) Applying EUV Double Patterning while maintaining the numerical aperture.

ii) Increasing the NA towards 0.5.

Recent studies of optical concepts presented during the last SPIE/BACUS conference showed that, when changing to higher NA, a change of demagnification of the imaging from the mask to the wafer plane is needed. This results in two potential implications:

- Either the photomask size is kept at the current 6 inches and the field size (printed on the wafer) needs to be reduced, or
- the (printed) field size is kept constant and the mask size needs to be increased to, let's say, 9 inches—"The Big Plates".

Both options have impact on the industry. Keeping the mask size at 6" would require a split design for today's single die devices and stitching the images. The change to 9" mask would require a new development of almost all mask manufacturing tools to handle the Big Plates. This implies that all mask manufacturing equipment starting from the mask-writer and ending with the mask-cleaner need to be redesigned or newly designed.

Furthermore, the mask makers need to switch to 9" masks for all layers of

(continues on page 7)

BACUS N • E • W • S

BACUS News is published monthly by SPIE for BACUS, the international technical group of SPIE dedicated to the advancement of photomask technology.

Managing Editor/Graphics Linda DeLano
Advertising Lara Miles
BACUS Technical Group Manager Pat Wight

SPIE

P.O. Box 10, Bellingham, WA 98227-0010 USA
Tel: +1 360 676 3290
Fax: +1 360 647 1445
www.SPIE.org
help@spie.org

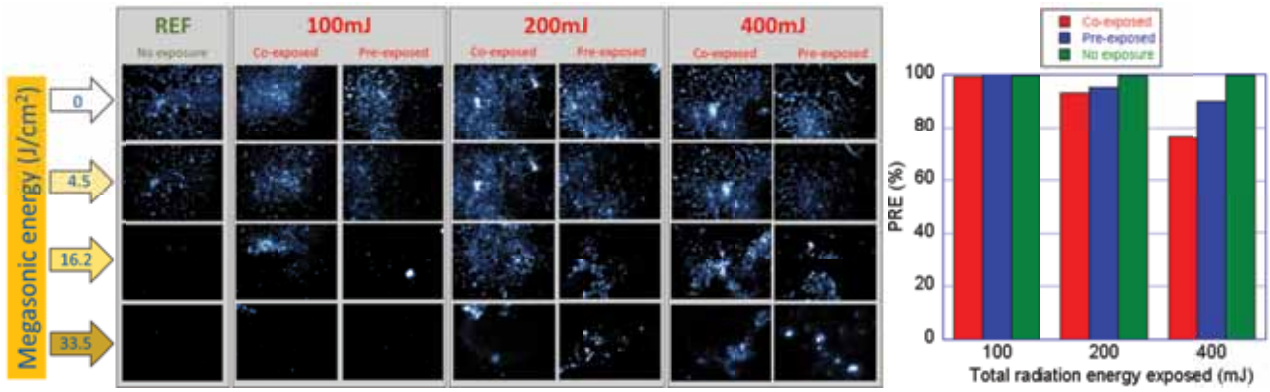

Figure 2. Results of radiation exposure experiments at λ=532 nm. The optical images of Ru-capped multilayer surfaces are shown for different radiation exposure powers and varied megasonic cleaning energy. Reference column represents the same plate, but not exposed to radiation. In the bar plot, PRE changes when varying radiation energy at λ=532 nm and megasonic energy of 33.5 J/cm² are shown.

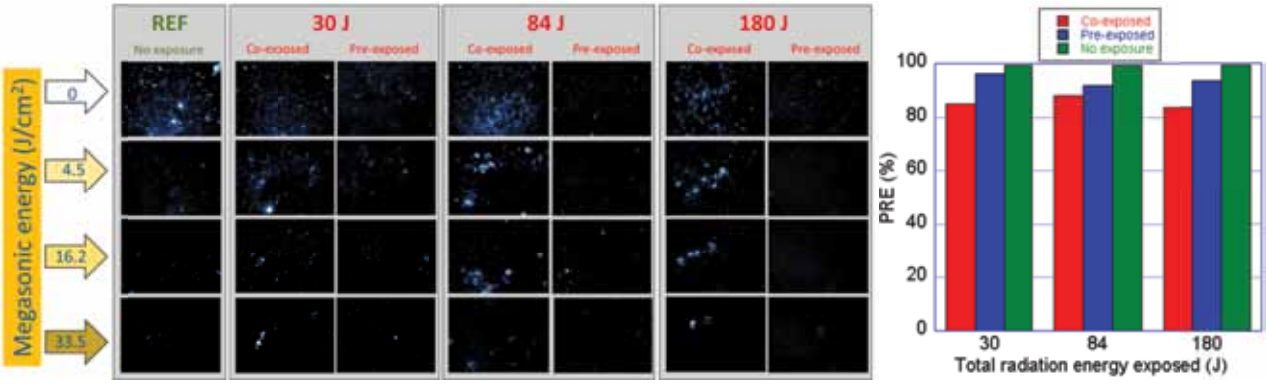

Figure 3. Results of radiation exposure experiments at λ=1064 nm. The optical images of Ru-capped multilayer surfaces are shown for different radiation exposure powers and varied megasonic cleaning energy. Reference column represents the same plate with no radiation exposure. In the bar plot, PRE changes when varying radiation energy at λ=1064 nm and megasonic energy of 33.5 J/cm² are shown.

the capping layer because it has good adhesion properties and is resistant to etching by chlorine chemistries, which makes it an ideal etchstop layer for the absorber. An EUV mask substrate coated with a MoSi ML and capped by Ru is typically called a ML blank. Although Ru is suitable for protecting MoSi MLs in harsh chemical and radiation environments, its stability during different processing conditions still poses some challenges. An EUV mask during its lifetime is exposed to radiation of different wavelengths and intensities. In addition to exposure at λ=11 nm to 14 nm during EUV lithography, the mask is also exposed to out-of-band (OOB) radiation with wavelengths of λ=200 nm to 600 nm originating at the EUV source.[1] Optical inspection tools expose EUV masks and blanks with (λ=193 nm to λ=488 nm) light. During cleaning, masks can also be exposed to 172 nm and/or 400 nm radiation. These radiation exposures can affect the material composition, surface energy, surface morphology, and surface defect properties of Ru-capped MoSi multilayer blanks. Depending on the power and the wavelength of the radiation, the changes may either be thermal or chemical, which may cause the multilayers to intermix, form silicide, and modify the different oxide phases.[2] Since these modifications occur close to the surface, the particle adhesion properties of Ru-capped MoSi multilayer blank surfaces are likewise affected.

Radiation-induced damage to MoSi multilayer mirrors has been studied using EUV to Near Infra-Red (NIR).[3-8] Our studies focused on chemical and physical modifications caused by varying the radiation energy. The research further explores radiation-induced modifications to particle adhesion on Ru-capped multilayer surfaces. Here we address the impact of radiation on EUV mask blank defectivity.

We previously demonstrated[2] that radiation can affect the surface structure of the Ru cap layer and form Ru silicide and/or Mo silicide phases with mixing ratios as a function of radiation energy. Radiation can also oxidize Ru and/or Si at the surface. As the material composition changes under exposure, the surface energy and roughness are likewise impacted. These physical properties may then result in different adhesion behaviors on the EUV mask surface. For

Table 1. Experimental parameters used in the radiation exposure experiments.

Wavelength (nm)	Laser power range	Exposure time (sec)	Total energy exposed (J)	Source
172	NA	NA	2.4	Excimer lamp
532	0.6-3.0 mW	130	0.1-0.4	Nd:YAG SHG
1064	0.5-3.0 W	60	30-180	Nd:YAG

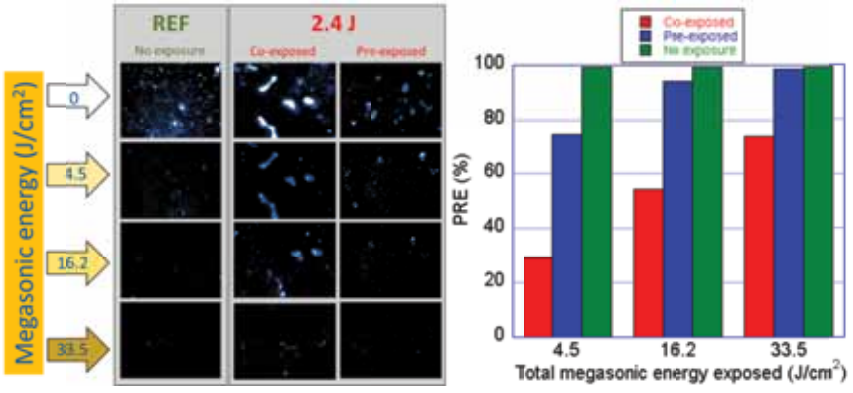

Figure 4. Results of radiation exposure experiments at λ=172 nm. a) The optical images of Ru-capped multilayer surfaces are shown for an exposure energy of 2.4J and varied megasonic cleaning energy. Reference column represents the same plate with no radiation exposure. The bar plot shows PRE changes when varying megasonic energy.

instance, a contaminant particle experiences a stronger adhesion force to a radiation-exposed surface than to a non-exposed (as-deposited) surface. However, if this contaminant particle is already on the mask surface during the radiation, in addition to the modifications to the physical properties of the surface, the interaction of the particle and surface is also impacted, which further increases surface adhesion. Understanding of both phenomena is essential to improve the stability, endurance, and lifetime of EUV masks.

2. Experimental Details

In these experiments, Ru-capped multilayer blank surfaces were exposed to optical radiation at λ=172 nm, λ=532 nm, and λ=1064 nm wavelengths. Optical microscopy was employed to study the adhesion properties of 10 µm polystyrene latex (PSL) particles deposited on the surface. The removal of these particles by standard cleaning process was used to obtain comparative information about their adhesion properties under different radiation conditions. Particles with stronger adhesion forces are obviously more difficult to remove, giving a lower particle removal efficiency (PRE) than particles that are easily removed. All radiation exposure experiments were done on different areas of a single Ru-capped ML blank to minimize variation resulting from the different surface properties of different blanks.

To study the effects of optical radiation on the adhesion properties of deposited particles, two sets of experiments were performed. In the first set (Fig. 1a), 10 µm PSL particles were deposited on blank surfaces and then exposed to radiation at different wavelengths. In the second set (Fig. 1b), the surface was exposed to radiation at different wavelengths before the 10 µm PSL particles were deposited. In both cases, cleaning processes with different particle removal efficiencies controlled by megasonic power were employed to remove the particles. A microscope with 40x magnification imaged the particles in a well-defined test area before and after cleaning. Particle counts were measured by analyzing the image captured at each step of the experiment. Particle removal efficiency was calculated by using particle counts at each of these steps. Megasonic energy was varied between 0 and 33.5 J/cm^2 at a fixed frequency of 1MHz. All steps were completed within 2 hours to minimize the dependence of particle adhesion on time.

For simplicity, “co-exposed” refers to the simultaneous exposure of the particle already on the surface (Fig. 1a) and “pre-exposed” indicates that the surface was exposed to radiation before the particle was deposited (Fig. 1b).

A pulsed Nd:YAG laser with a repetition rate of 10Hz and a pulse width of 10 ns was used for λ=1064 nm radiation and its second harmonic was used for λ=532 nm. The exposure time and power were adjusted to ensure precise exposure energy. For radiation exposure at λ=172 nm, an Ushio excimer UV lamp system was used and the surface was purged with N2 during exposure. Here, the energy applied to the surface was calculated from exposure time and radiation power was measured by an internal sensor in the lamp assembly. The power range, exposure time, and total exposure energy for each case are given in Table 1.

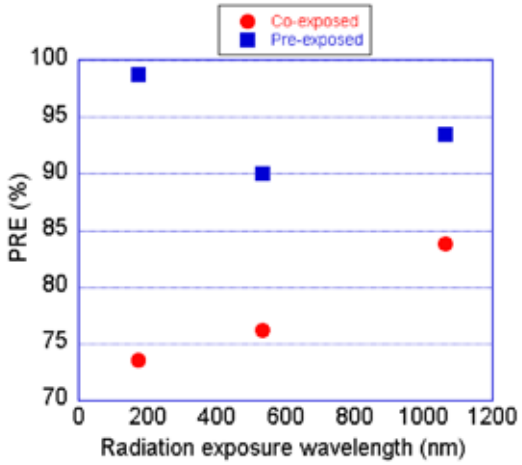

Figure 5. Comparison of the PRE obtained at different wavelengths with a megasonic energy of 33.5 J/cm².

3. Radiation Exposure

Figure 2 shows micrographs of the radiation exposure experiments at λ=532 nm with three different energies: 100mJ, 200mJ, and 400mJ. These values are the total amounts delivered to the surface. For each exposure step, two different areas were exposed: the surface with particles (co-exposed) and the surface without particles (pre-exposed). The micrographs are labeled accordingly. The reference column (REF) shows a micrograph of the particles in the areas that were not exposed to radiation. The micrographs of the particles captured after each cleaning step are shown in the rows labeled with corresponding total megasonic energy: 0 J/cm² as the target reference, 4.5 J/cm², 16.2 J/cm², and 33.5 J/cm². These values are the total megasonic energies delivered to the target surface.

The bar plot in Figure 2 shows PRE in relation to the radiation exposure energy for a cleaning process with a maximum megasonic power at 33.5 J/cm² (corresponding to the last row of the optical images); the pre-exposed and co-exposed surfaces are labeled accordingly. For the non-exposed area (REF), the PRE is high (>99%). However, under radiation, the PRE drop as a function of the exposure energy at λ=532 nm, indicating that radiation at λ=532 nm will increase the particle adhesion to the Ru-capped surface and a minimum radiation energy is required to modify this particle adhesion. However, particle adhesion is stronger when particles are initially on the surface (co-exposed) than when they are deposited after exposure to λ=532 nm (pre-exposed). In the latter case, we have observed[2] that exposure of the surface to 532 nm light with the same energy oxidizes the Ru surface and RuO_2 tends to form rather than other Ru oxide valences. In addition to the change in the Ru oxidation valance on the surface, surface energy can also change. The mechanisms involved in increasing PSL particle adhesion to the Ru cap surface under 532 nm radiation are still under investigation. Potential chemical bonding between polystyrene and Ru or another interaction may play a role in increasing adhesion. However, no thermal effects are expected to directly contribute to increased particle adhesion since the thermal effects occur before particle deposition and they only modify the surface.

When the same surface with already deposited particles (co-exposed) was exposed to the same radiation energies, the PRE is less than pre-exposed surfaces, indicating that co-exposure increases adhesion. In this case, radiation-induced surface modification contributes to adhesion similar to the pre-exposed experiment. However, simultaneous exposure of the PSL particle and the surface may promote potential chemical bonding or deform the particle, thereby increasing the contact area between the particle and Ru surface. Experiments are in progress to verify this hypothesis.

Figure 3 shows the results of the radiation exposure experiments at λ=1064 nm. Three different exposure energies were studied at 30J, 84J, and 130J with pulsed exposures at 0.5W, 1.5W, and 3W. The energy values are the total amounts delivered to the surface within 60 seconds at the given laser powers. Note that the applied exposure energy is substantially (more than 2 orders of magnitude) higher than the energy applied at λ=532 nm while all other steps in these experiments are the same as those experiments at λ=532 nm. Both λ=532 nm and λ=1064 nm experiments were performed on the same Ru-capped blank.

The optical images shown in Figure 3 were processed using the same procedure as was used for the experiments at λ=532 nm. The results are shown for the maximum megasonic exposure at 33.5 J/cm² in the bar plot. For each radiation level, PRE is grouped according to co-exposed, pre-exposed, exposures, and reference. Similar to λ=532 nm, the non-exposed (REF) area had a high PRE; however, the PREs for both pre-exposed and co-exposed areas are relatively higher and do not depend on the exposure energies used in these experiments. This is probably because the exposure energy was much higher than was used with

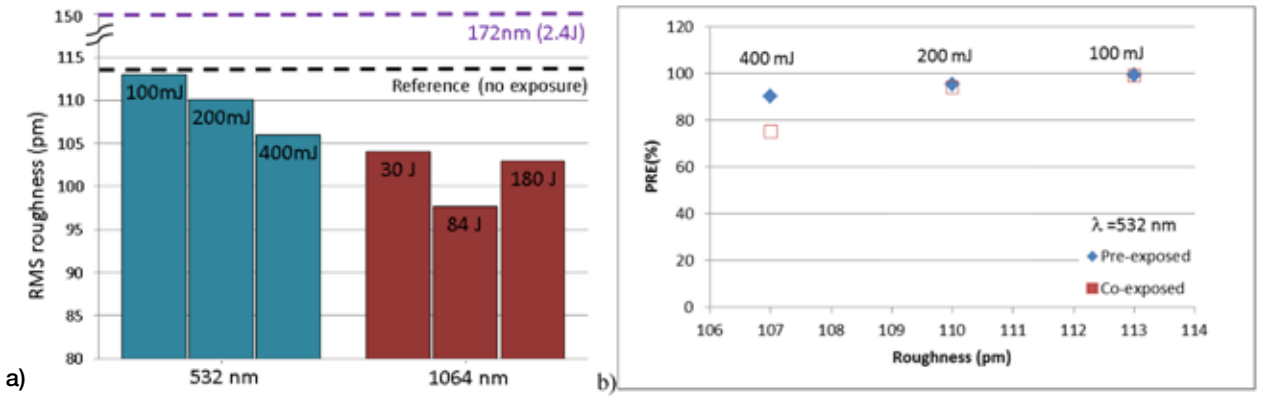

Figure 6. Surface roughness changes are shown for different radiation wavelengths.

λ=532 nm. Hence, particle adhesion under λ=532 nm and λ=1064 nm exposure is similar and co-exposure produced a high adhesion force than pre-exposure. Furthermore, with high exposure energies (λ=1064 nm, 30J to 180J), particle adhesion does not appear to depend on exposure energy.

Figure 4 shows the results of experiments at λ=172 nm. Here, constant radiation energy was delivered by an excimer UV lamp at 2.4J and PRE was calculated for megasonic energies of 4.5 J/cm^2, 16.2 J/cm^2, and 33.5 J/cm^2. The PREs for all cleaning energies are shown in the bar plot next to the optical images. PRE for pre-exposed and non-exposed surfaces are similar, but the co-exposed surface exhibited a much lower PRE.

The effect of λ=172 nm radiation has been extensively studied by SEMATECH and others. The Ru surface can be oxidized under exposure to λ=172 nm and with the gas atmosphere used during radiation. In some cases, Si on the surface is also oxidized. In addition, the photon energy at λ=172 nm is high and will therefore break the carbon double bond in the PSL structure as well as PLS cross links on the surface. As a result, these particles will deform and become difficult to remove.

Figure 5 compares the measured PRE after radiation exposure at different wavelengths (172 nm (2.4J), 532 nm (400 mJ), and 1064 nm (180J)) with a megasonic energy of 33.5 J/cm^2. For pre-exposed surfaces, the PRE becomes slightly less as the wavelength increases. Note that the change in PRE is not statistically significant for λ=532 nm λ=1064 nm; however, for λ=172 nm, it is somewhat higher, which may be due to greater surface roughness caused by oxidation or chemical surface interactions. For co-exposed surfaces, PRE exhibits a monatomic increase when the radiation wavelength increases. Different mechanisms are responsible for this behavior. Higher energy photons in shorter wavelengths lead to solarization, cross linking, and deformation of PSL particles, making them difficult to remove. However, the exact mechanism that changes surface adhesion under λ=532 nm and λ=1064 nm exposure is not well understood and currently is under investigation. Our time-of-flight secondary ion mass spectroscopy (TOFSIMS) study[2] shows the chemical structure of the Ru oxide is modified at the surface or close to the surface. Currently, we are studying thermal effects on PSL particles on the surface and potential PSL deformation under exposure to λ=1064 nm light.

In Figure 6.a, surface roughness is shown as a function of total radiation energy at different exposure wavelengths. Surface roughness depends on radiation exposure energy. The surface roughness of typical Ru-capped MLs made by SEMATECH before exposure is about R_a= 112 pm (RMS). Exposure to λ=172 nm oxidizes the surface, dramatically increasing surface roughness to R_a= 150 pm (RMS). However, with λ=532 nm light when the total exposure energy is below 500 mJ, surface roughness monolithically decreases toward R_a= 105 pm (RMS), making the surface smoother. Finally, in the high energy regime (30J to 180J) with λ=1064 nm, surface roughness remains constant around R_a= 100 pm (RMS), which is close to the surface roughness of the EUV substrate (i.e., under the multilayer). Surface roughness was measured multiple times to ensure measurement repeatability. The atomic force microscope (AFM) used at SEMATECH has a noise floor of about 40 pm, which indicates the lower roughness measurement value of this tool. Therefore, any change on the order of 5 pm should be measurable. Further experiments on different blanks are still needed to validate changes in surface roughness in this regime.

PRE is compared to surface roughness under λ=532 nm light in Fig.6.b. PRE is apparently less for smoother surfaces, which agrees with our expectations since smoother surfaces have a larger contact area, making it more difficult to remove particles. Again, further experiments are needed to confirm changes in surface roughness by a few pm.

4. Conclusion

The effects of radiation on particle adhesion properties of Ru-capped MoSi multilayers have been studied using optical wavelengths. Regardless of the wavelength of the radiation used on a surface with or without particles, the surface adhesion of defects increased under exposure

to radiation and scaled with laser power. While adhesion increases largely because of the optical absorption of defects at λ=172 nm, exposure at λ=532 nm caused both absorption and chemical modification of the Ru surface. At 172 nm, PRE decreases about 25%, indicating the greatest increase in adhesion of pre-existing defects. For surfaces without defects, radiation did not induce any significant change in surface adhesion properties, but surface roughness increased. Therefore, surface treatment under VUV will not negatively impact defectivity. However, with existing defects, moderate VUV powers must be used and cleaning parameters must be adjusted accordingly. For λ=532 nm, although low laser powers were used, PRE degraded > 20%, with equal contributions from chemical modification of the surface and particle absorption. At 532 nm, by increasing the radiation energy, surface roughness decreased, which may have increased surface adhesion because of the larger contact area. For λ=1064 nm, similar to 532 nm, both chemical modification and particle absorption contribute to greater absorption. Because of the very high laser power used at this wavelength, the smoothest surfaces were measured at 1064 nm exposure. In conclusion, further studies on the relation of radiation exposure and mask defectivity are required to improve Ru-capped MoSi multilayer masks.

5. References

[1]. O. Morris *et al.*, "Extreme ultraviolet and out-of-band radiation emission from a tin droplet based LLP source," **Proc. of SPIE,** Vol. 8322, 83220I, (2012).

[2]. A. Rastegar *et al.*, "Effect of radiation on the defectivity and stability of Ru-capped MoSi multilayer blanks," **Proc. of SPIE,** Vol. 8322, 832211, (2012).

[3]. M. Müller *et al.*, "EUV damage threshold measurements of Mo/Si multilayer mirrors," **Appl. Phys. A,** Vol. 108, 2, 263-267, (2012).

[4]. K. Mann *et al.*, "Damage testing of EUV optics using focused radiation from a table-top LLP source," **Proc. of SPIE,** Vol. 7969, 796926 (2011).

[5]. E. Louis *et al.*, "Damage studies of multilayer optics for XUV Free Electron Lasers," **Proc. of SPIE,** Vol. 7361, 73610I (2009).

[6]. F. Barkusky *et al.*, "Damage threshold measurements on EUV optics using focused radiation from a table-top laser produced plasma source," **Opt. Express,** Vol. 18(5), 4346-4355 (2010).

[7]. A. Giglia *et al.*, "EUV soft x-ray characterization of a FEL multilayer optics damaged by multiple shot laser beam," **Nucl. Instr. and Meth. in Phys. Res. Sec. A,** Vol 635, 1, Supp., S30-S38, (2011).

[8]. M. Suman *et al.*, "Analysis of the damage effect of femtosecond-laser irradiation on extreme ultraviolet Mo/Si multilayer coating," **Thin Solid Films,** Vol. 520, 6, 2301-2306, (2012).

EDITORIAL *(continued from page 2)*

a reticle set including the Big Plates. For non-critical layers, the Mix-and-Match scenarios in wafer fabs and mask design need to consider different mask sizes and the impact of different mask manufacturing tools on registration and CD control.

Mask equipment manufacturers need to start planning now the projects for newly designing the tools and to start looking for funding to develop this completely new equipment for a rather limited market.

Since this is a major endeavor, there needs to be a fast building of consensus by the key players that adopt EUV giving us a decision in a timely manner: Are we voting for the "Big Plates" - yes or no? It might be worthwhile to form a Steering Committee to foster the decision.

BACUS N • E • W • S

Industry Briefs

Brewer Science introduces CNT inks for printed electronics

Solid State Technology, Nov 15, 2012

Rolla, MO-based Brewer Science introduced a line of conductive CNT ink materials that are surfactant free, require no additional rinse steps, and are compatible with a broad range of printed electronic substrates. Cure temperatures for desired conductivity results are between 115°C and 130°C. Inks with high concentrations of CNTs in low-viscosity solutions are available in aqueous and solvent-based systems, giving them broad compatibility and enabling the design of inks for a broad set of application technologies such as sensors, displays, and packaging integration. Formulations are available for Optomec's Aerosol Jet® technology systems, Fujifilm Dimatix's materials printer DMP-2800, spray coating, and drawdown bar coating. These CNT inks have achieved sheet resistance of 300 ohm/sq for 85%T (optical transmission) at 550 nm for transparent conductive applications. For conductive trace applications, sheet resistance of 1 ohm/sq and conductivity of 75,000 siemens/meter have been achieved. Films produced with these inks on polyethylene terephthalate (PET) have demonstrated both high adhesion and mechanical flexibility, stable after repeated folding of the CNT-coated PET.

"This robust performance will enable flexible printed electronic device applications," "These solutions contain no surfactants and require no additional post-process rinsing, which will speed commercial adoption," said Jim Lamb, Director of Brewer Science's Printed Electronics Technology Center. "Although we designed these materials for plastic printed electronics applications, they are also compatible with a wide range of substrates such as paper, glass, silicon, and metal." Brewer Science is focused on bringing the unique properties of CNTs for commercial electronics applications to customers in the next three to five years.

Process Watch: Taming the overlay beast

Rebecca Howland, Amir Widmann, KLA-Tencor

Controlling overlay error is one of the most difficult issues that lithography engineers face. The overlay may include mask pattern placement error, deviations from wafer planarity, scanner nonlinearities and process variation. In most cases, it is measured optically by capturing an image of a specially designed alignment mark called an overlay target. Half of the overlay target is printed during the first process step, and the other half of it is printed during the second process step. The result is reported as a vector quantity, having a magnitude and direction corresponding to the x and y offsets.

A recent development in the area of overlay measurement is extension of measurement capability to new layers and new materials. The metrology tool needs to be able to send photons through the top layer to detect the pattern underneath, and the quality of the image of the buried pattern is critical to the quality of the overall measurement. Because semiconductor processes use a variety of materials, and the optical absorption of a given material generally varies with wavelength, the well-equipped metrology system can select from a variety of wavelengths to achieve sufficient image quality for the buried pattern to enable an accurate, repeatable measurement. The alternative—introducing an extra process step to etch a "window" in the top layer before patterning it—adds significant cycle time and may degrade the underlying pattern. Examples of particularly challenging classes of materials are those used to build 3D transistors, and hard mask materials used during litho-etch-litho-etch lithography. The latest overlay metrology systems can provide an appropriate wavelength that penetrates the top layer, making overlay metrology feasible without additional process steps.

Another new development in the field of overlay metrology is the use of multi-layer overlay targets. New target designs now allow a lithography engineer to measure within-layer overlay and between-layer overlay using one target. These innovative targets are small enough to be inserted into the die without consuming an unfeasible amount of valuable real estate. Their designs are flexible and robust, allowing adjustments for specific process and layer requirements. The new multi-layer targets allow lithographers to measure within- and between-layer overlay error with one image and, at the same time, reduce systematic errors that could degrade the measurement if separate targets had been used.

Synopsys and TSMC Enable Lithography Compliance Checking for 20nm

Mountain View, Calif., Nov. 14, 2012. Synopsys, Inc. announced the delivery of lithography compliance checking technology for the TSMC 20-nanometer (nm) DFM Data Kit (DDK) encapsulated with Synopsys® Proteus mask synthesis technologies. As a result of the design-for-manufacturing collaboration between TSMC and Synopsys, the compliance checking engine in the DDK helps designers identify lithography-related problems early in the design development phase, avoid litho-related manufacturing issues and late-stage schedule slips resulting from re-design.

The TSMC 20-nm DDK complements traditional physical verification rules with a highly accurate simulation-based solution to identify design non-compliance using a direct simulation of the manufacturing process. Lithography correction and verification tools used in the manufacturing mask synthesis flow are embedded in the DDK, resulting in accurate hotspot detection.

"We share TSMC's commitment to the success of our mutual customers and look forward to continuing to provide the latest software technology supporting most advanced technology nodes," said Tom Ferry, senior marketing director of the Silicon Engineering Group at Synopsys. "Our close collaboration to develop the 20-nanometer DDK helps bridge the gap between design and manufacturing, enabling faster volume ramps and more predictable product release cycles."

"The 20-nanometer DDK gives designers access to simulation-based hotspot detection, so they can efficiently identify out of compliance areas and take corrective action before manufacturing." said Suk Lee, senior director of Design Infrastructure Marketing at TSMC.

Join the premier professional organization for mask makers and mask users!

About the BACUS Group

Founded in 1980 by a group of chrome blank users wanting a single voice to interact with suppliers, BACUS has grown to become the largest and most widely known forum for the exchange of technical information of interest to photomask and reticle makers. BACUS joined SPIE in January of 1991 to expand the exchange of information with mask makers around the world.

The group sponsors an informative monthly meeting and newsletter, BACUS News. The BACUS annual Photomask Technology Symposium covers photomask technology, photomask processes, lithography, materials and resists, phase shift masks, inspection and repair, metrology, and quality and manufacturing management.

Individual Membership Benefits include:

- Subscription to BACUS News (monthly)
- Complimentary Subscription *Semiconductor International* magazine
- Eligibility to hold office on BACUS Steering Committee

www.spie.org/bacushome

Corporate Membership Benefits include:

- Three Voting Members in the SPIE General Membership
- Subscription to BACUS News (monthly)
- One online SPIE Journal Subscription
- Listed as a Corporate Member in the BACUS Monthly Newsletter

www.spie.org/bacushome

Calendar

2013

SPIE Advanced Lithography

24-28 February 2013
San Jose Convention Center and
San Jose Marriott
San Jose, California, USA
www.spie.org/al

SPIE Photomask Technology

10-12 September 2013
Monterey Marriott and
Monterey Conference Center
Monterey, California, USA
www.spie.org/pm

SPIE is the international society for optics and photonics, a not-for-profit organization founded in 1955 to advance light-based technologies. The Society serves nearly 225,000 constituents from approximately 150 countries, offering conferences, continuing education, books, journals, and a digital library in support of interdisciplinary information exchange, professional growth, and patent precedent. SPIE provided over $2.7 million in support of education and outreach programs in 2011.

SPIE

International Headquarters
P.O. Box 10, Bellingham, WA 98227-0010 USA
Tel: +1 360 676 3290
Fax: +1 360 647 1445
help@spie.org • www.SPIE.org

Shipping Address
1000 20th St., Bellingham, WA 98225-6705 USA

SPIE Europe
2 Alexandra Gate, Ffordd Pengam, Cardiff,
CF24 2SA, UK
Tel: +44 29 2089 4747
Fax: +44 29 2089 4750
spieeurope@spieeurope.org • www.spieeurope.org

You are invited to submit events of interest for this calendar. Please send to lindad@spie.org; alternatively, email or fax to SPIE.